J|A|C|S COMMUNICATIONS

Published on Web 03/06/2009

Amphiphilic TiO_2 Nanotube Arrays: An Actively Controllable Drug Delivery System

Yan-Yan Song, Felix Schmidt-Stein, Sebastian Bauer, and Patrik Schmuki*

Department of Materials Science, WW4-LKO, University of Erlangen-Nuremberg, Martensstrasse 7 D-91058, Erlangen, Germany

Received January 8, 2009; E-mail: Patrik.Schmuki@ww.uni-erlangen.de

In 1999, the formation of self-organized arrays of TiO_2 nanotubes by electrochemical anodization of Ti was reported by Zwilling and co-workers.[1] Since then, TiO_2 nanotube arrays have generated much interest because of the combination of geometric features with the unique functional properties of TiO_2 (for a recent review, see ref 2). A key feature of TiO_2 is its excellent photocatalytic properties,[3] which are significantly enhanced for nanotubular structures.[4] This not only allows the controlled decomposition of organic materials[5,6] but also allows the highly controlled scission of surface attached organic monolayers.[7,8] Moreover, TiO_2 nanotubes show excellent biocompatibility,[9,10] and therefore the open volume in the tubes may be exploited as a drug release platform. However, when the drug is simply filled into a porous network or tubes (for example to be used on a titanium implant or bone-filling material[11−13]), a main problem is the uncontrolled release of drugs or therapeutics. Therefore, providing a controlled release kinetics is a key objective of many novel drug delivery approaches,[14,15] and as a result, over the past few years, new structures,[9] surface modification,[13,16] and release principles have been widely explored. Hydrophobic surface modifications are typically used to avoid undesired nonspecific adsorption of critical proteins (e.g., bovine serum albumin)[17] to the drug delivery device. In this context, also amphiphilic structures attract considerable attention, as they for example allow combining a hydrophilic drug with a hydrophobic surface.

In the present work, we demonstrate the fabrication and use of an amphiphilic TiO_2 nanotubular structure that provides a highly controllable drug release system based on a hydrophobic cap on a hydrophilic TiO_2 nanotube. This hydrophobic cap prevents uncontrolled leaching of the hydrophilic drug into an aqueous environment. By exploiting the photocatalytic nature of TiO_2 for UV induced chain scission of attached organic monolayers, the cap can be removed and a highly controlled release of drugs can be achieved.

Figure 1 schematically describes the procedure for the fabrication of amphiphilic TiO_2 nanotubes (Figure 1A) and drug loading approaches explored in this work (Figure 1B). To produce amphiphilic tubes, the procedure consists of a first anodization step forming tubes, followed by a hydrophobic surface modification. Then, a second neat (hydrophilic) tube layer is grown underneath the first one by a second anodization process. The first tube layer was grown in a glycerol/water/NH_4F[18] electrolyte to a thickness of ~750 nm with individual nanotube diameters of ~90 nm (Figure 2). Then a hydrophobic monolayer of octadecylphosphonic acid (OPDA) was attached to the tube walls. The sample is then anodized again in an ethylene glycol/NH_4F electrolyte (experimental details are given in the Supporting Information SI X1). In contrast to water-based electrolytes, ethylene glycol electrolytes enter into the hydrophobic tubes and therefore allow for a second anodization. The voltages for anodization were chosen to match the nanotube diameter in the first and second layers.[19−21] In our case, the second

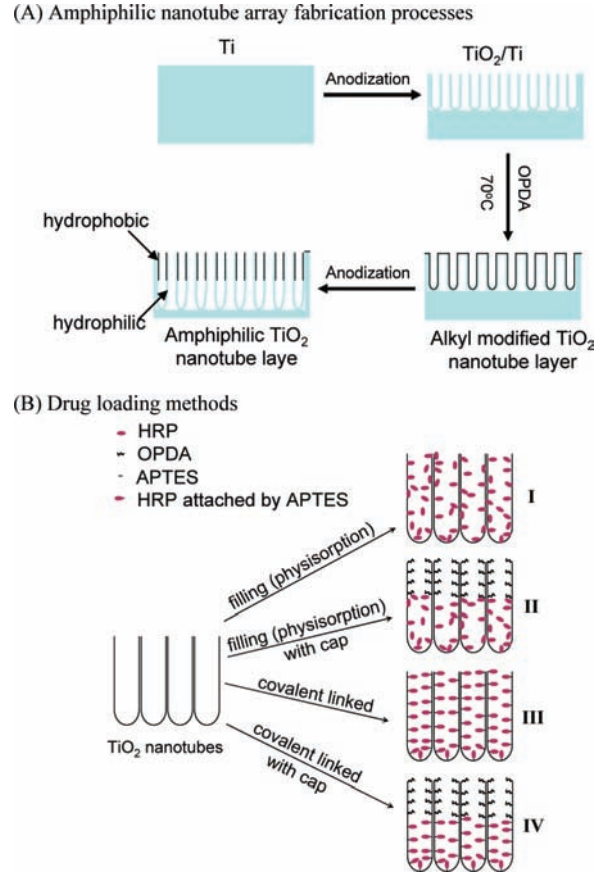

Figure 1. (A) Scheme of the procedure for fabricating amphiphilic TiO_2 nanotube layers, and (B) four methods for drug loading using horseradish peroxide (HRP) as a hydrophilic model drug: (I) immersion without any TiO_2 surface modification (for reference), (II) immersion after OPDA modification in the upper nanotube layer (hydrophobic cap), (III) covalently attached HRP over the entire nanotube layers, (IV) OPDA cap in the upper nanotube layer and covalently attached HRP in the lower nanotube layer. Surface analytical support for the processes is provided in SI X3.

layer consists of 2 μm long tubes (Figure 2B) with a diameter of ~90 nm (inset of Figure 2A). To evaluate the growth of the second layer after the first layer has been formed, we performed detailed scanning electron microscopy (SEM) characterization of the interface between the layers, with examples shown in Figure 2C and D. From these investigations it is clear that the second anodization penetrates the bottom of the tubes grown during the first anodization,[19−21] and tube growth (Figure 2C and D) is re-established. This implies that field-induced breakdown of the monolayer occurs only at the tube bottom. After growth has been re-established, the length of the underneath tubes can simply be controlled by the anodization time.

10.1021/ja810130h CCC: $40.75

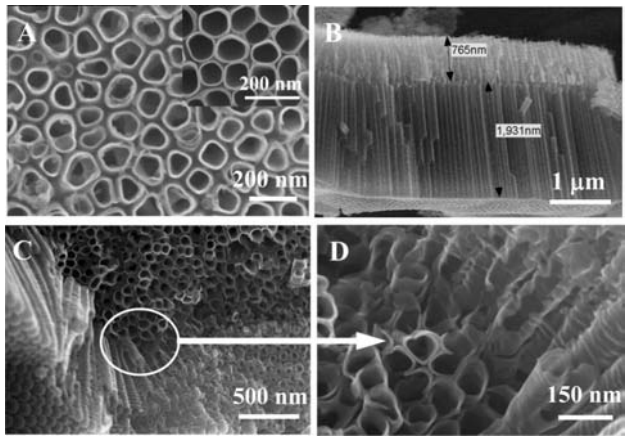

Figure 2. SEM top-view images of the first nanotube layer (A) and the second nanotube layer (inset of A), cross-sectional image for the double nanotube layers (B), and cross-sectional images of the interface between the upper and the lower TiO_2 nanotube layers (C) and (D).

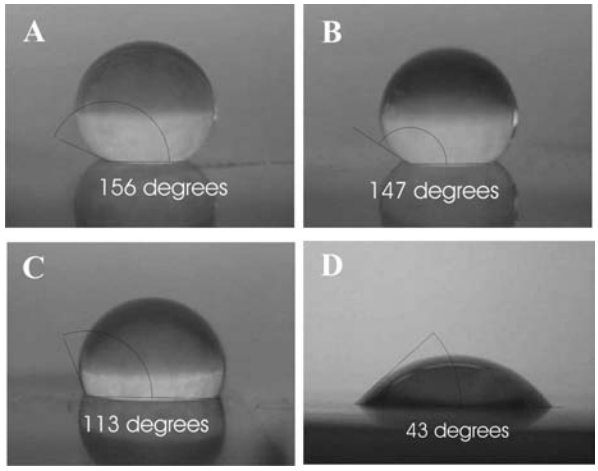

Figure 3. Optical images of a water droplet on TiO_2 nanotube layers: (A) after modification with OPDA monolayers, (B) after the second anodization, (C) after HRP grafting, (D) after releasing HRP by UV illumination for 10 min.

As-grown TiO_2 nanotube arrays show water contact angles close to 0° without any modification to the surface, reflecting the completely hydrophilic behavior of these TiO_2 surfaces.[7,22] However, the surface can be modified with organic monolayers using functional groups, such as phosphates, carboxylates, or silanes.[22−24] In the present work, to produce the hydrophobic top part of the tubes, OPDA is grafted to the outer tube layer after the first anodization step. As shown in Figure 3A, the surface wettability with OPDA monolayer grafting changes from superhydrophilic to superhydrophobic with a contact angle $\theta = 156°$. After the second anodization in the lower part, a new hydrophilic surface is created, but the contact angle of the surface remains hydrophobic with $\theta = 147°$ (Figure 3B). This shows that although a slight decrease in the contact angle occurs (monolayer deterioration), still the hydrophobic outer nature is maintained; i.e., the OPDA monolayer in the first layer can largely "withstand" the second anodization step in the fluoride-containing electrolyte.

To exploit the amphiphilic nanotube arrays in the form of hydrophobically capped carriers for hydrophilic drugs, different drug loading approaches were explored, as outlined in Figure 1B. For reference, unmodified double anodized tubes were loaded by simple immersion in our model drug system [a solution of horseradish peroxidase (HRP); see SI1 for details] (Figure 1B, case I). This

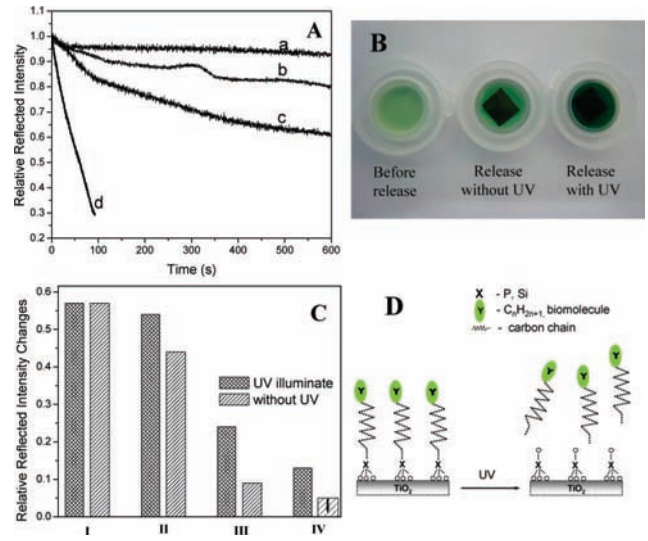

Figure 4. Drug release: (A) Relative intensity of reflected light (wavelength 550 nm) as a function of time after exposure of HRP loaded amphiphilic nanotubes to PBS without illumination (curve a), 50% UV illumination (curve b), and full UV illumination (curve c). Curve d shows the release of HRP in TiO_2 nanotubes without any surface modification (reference curve). (B) Optical images of the solution containing indicator substrate (ABTS) and H_2O_2 before HRP release (left) and after HRP release without (middle) and with UV illumination for 40 min (right). (C) Relative reflected intensity changes for the four different types of nanotubes used in this study (according to the scheme of Figure 1B) with and without UV illumination. (D) Scheme of the HRP release under UV illumination. (Additional release experiments are shown in SI X1 and SI X2: supporting surface analytical data are given in SI X3.)

simply leads to free and physisorbed drug molecules within the tubes. In the second approach (Figure 1B, case II), capped tubes (where the upper part carried the OPDA monolayer) were immersed in HRP (the aqueous solution containing HRP can infiltrate into the tubes, because of the presence of DMSO that acts as a surfactant). This approach also leads to free (physisorbed) HRP molecules in the lower part of the tubes, but after evaporation of the DMSO, the HRP remains trapped by the hydrophobic cap. In the third approach (Figure 1B, case III), no hydrophobic cap was present, and the HRP was grafted as outlined in SI1 on all of the hydrophilic tube walls by an APTES/vitamin C monolayer linker. In the fourth approach (Figure 1B, case IV), we used the OPDA cap and also attached the HRP to the lower part of the tube wall as in case III. After loading, all samples were dried by a N_2 flow, followed by washing with 50 μL of PBS (physiological body solution). The entire treatment with APTES and HRP loading resulted in a changed water contact angle to 113° (Figure 3D). The decrease of contact angle originates from the defects in the first OPDA layer that are formed during the entire processing of the lower layer. These defects offer some potential positions for (unwanted) HRP binding in the upper tube part. However, this lowering of the contact angle does not significantly affect the operation of the principle as we will show below. To explore the use and release of the immobilized or loaded enzyme from the tubes, a colorimetric reaction was used. Using a visible light spectrometer, the HRP release was monitored by the light absorption changes in a beaker setup as shown in Figure 4B. Here, 0.4 mL of PBS solution containing 0.3% H_2O_2 and 0.05 M 2,2′-azino- bis(3-ethylbenzothiazoline-6-sulfonic acid) diammonium salt (ABTS) as the HRP release indicator were used as the surrounding solution. The intensity of the reflected light, from the TiO_2 nanotube sample placed at the bottom of the beaker, was measured at a wavelength of 550 nm.[26] The reflectivity decreases as the blue enzymatic oxidation product

of ABTS is produced in the initially light green solution. To demonstrate photocatalytic control of the release, we carried out experiments with and without UV-light illumination ($\lambda = 325$ nm, He−Cd Laser, Kimmon, Japan, defocused to an intensity of ~50 mW/cm^2).

The HRP release characteristics for the different loading approaches are compared in Figure 4. In Figure 4A, curves a, b, and c correspond to amphiphilic nanotubes, where HRP molecules were attached (linked) to the lower tube part. Curve d represents the case when neither cap nor linker is used (HRP filled hydrophilic TiO_2 nanotubes without any modification). The results show clearly that the release rates are strongly different for the different kinds of nanotubes. If the HRP is only loaded by dipping, a quick and uncontrollable release is obtained. Almost 90% of the molecules release in the first minute (Figure 4A, curve d, with a kinetic constant $k = 1.32 \times 10^{-2}$ s^{-1}). For the OPDA capped nanotubes and surface linked HRP, the release rate can be adjusted by UV illumination (Figure 4A, curve b is taken at 50% light intensity of case c). Clearly, a higher UV intensity results in a faster release rate than lower UV intensity (in fact the kinetic constants $k_c = 8.21 \times 10^{-4}$ s^{-1} and $k_b = 3.74 \times 10^{-4}$ s^{-1} correlate directly with the light intensity under the present conditions). Figure 4B shows visually the color change for the solution after HRP release from OPDA and APTES modified amphiphilic nanotubes for 40 min with and without UV illumination. In Figure 4C, we compare the release kinetics for the four kinds of HRP-filled nanotubes as shown in Figure 1B (I−IV).

The amphiphilic nanotube layers with OPDA (hydrophobic cap) and covalently linked HRP (case IV) clearly allow the largest degree of UV illumination controllable release (note: the reflected light intensity without UV illumination was in this case within the error bar of the detection limit). In line with a successful release (removal of the protective cap), a strong change in surface wettability can be detected after the UV illumination, as shown in Figure 3D. When the bonds are broken by UV illumination, the hydrophobic OPDA molecules on the first nanotube layer are decomposed; at the same time also the APTES linker is cut and HRP can diffuse into the solution. The results also show clearly that the hydrophobic cap highly efficiently prevents leaching of the HRP or the influx of the aqueous surrounding media (as in experiments for several hours no significant color change can be observed under dark conditions). According to the data provided in the Supporting Information (SI X3) and in line with literature dealing with UV-induced decomposition of organic monolayers on flat and nanotubular TiO_2 surfaces,[3,7,27] it can be expected as outlined in Figure 4D that UV illumination causes APTES or phosphonate chain scission directly after the polar group, i.e., Si or P, leaving the polar group on the surface, cutting off the aliphatic tails, and releasing the aliphatic rest and HRP molecules into the solution. Furthermore, additional experiments (see Supporting Information SI X1) confirmed that the HRP release is faster than photocatalytic HRP destruction; i.e., the activity is to a large degree maintained.

In conclusion, amphiphilic TiO_2 nanotubes are fabricated by a double anodization procedure combined with organic monolayer grafting. These tubes can be used as "capped" biomolecule carriers with ~4.4×10^{-11} nmol per tube. By utilizing the excellent photocatalytic ability of TiO_2, the controllable release for enzyme molecules and a large range of proteins (that all can be attached using the universal treatment of ref 25) can be achieved. A key feature is the loss of the nonpolar part of the OPDA molecule that changes the wettability to hydrophilic. Once the pore surface is sufficiently hydrophilic, capillary forces will allow the entry of the environment and the release of the payload. Additionally, the amphiphilic characteristics with the hydrophobic outside provides a surface condition counteracting nonspecific protein adsorption.[17] It should furthermore be mentioned that in view of in vivo applications it has also been found that chain scission induced release from TiO_2 surfaces can be triggered not only by UV light but also by suitable X-ray radiation,[28] thus opening potential perpectives for invasion-free use of the principle.

Acknowledgment. This work was supported by grants from the DFG (Cluster of Excellence) and the Alexander von Humboldt Foundation of Germany.

Supporting Information Available: Experimental details. This material is available free of charge via the Internet at http://pubs.acs.org.

References

(1) Zwilling, V.; Darque-Ceretti, E.; Boutry-Forveille, A. *Electrochim. Acta* **1999**, *45*, 921–929.
(2) Ghicov, A.; Schmuki, P. *Chem. Commun.*, accepted.
(3) Wang, R.; Hashimoto1, K.; Fujishima, A.; Chikuni, M.; Kojima, E.; Kitamura, A.; Shimohigoshi, M.; Watanabe, T. *Nature* **1997**, *388*, 431–432.
(4) Macak, J. M.; Zlamal, M.; Krysas, J.; Schmuki, P. *Small* **2007**, *3*, 300–304.
(5) Paramasivalm, I.; Macak, J. M.; Schmuki, P. *Electrochem. Commun.* **2008**, *10*, 71–75.
(6) Paramasivalm, I.; Macak, J. M.; Ghicov, A; Schmuki, P. *Chem. Phys. Lett.* **2007**, *445*, 233–237.
(7) Balaur, E.; Macak, J. M.; Taveiraa, L.; Schmuki, P. *Electrochem. Commun.* **2005**, *7*, 1066–1070.
(8) Shrestha, N. K.; Macak, J. M.; Stein, F. S.; Hahn, R.; Mierke, C. T.; Fabry, B.; Schmuki, P. *Angew. Chem., Int. Ed.* **2009**, *48*, 969–972.
(9) Park, J.; Bauer, S.; von der Mark, K.; Schmuki, P. *Nano Lett.* **2007**, *7*, 1686–1691.
(10) von Wilmowsky, C.; Bauer, S.; Lutz, R.; Meisel, M.; Neukam, F. W.; Toyoshima, T.; Schmuki, P.; Nkenke, E.; Schlegel, K. A. *J. Biomed. Mater. Res., Part B* **2008** Sep 8.,in print.
(11) Mani, G.; Johnson, D. M.; Marton, D.; Feldman, M. D.; Patel, D.; Ayon, A. A.; Agrawal, C. M. *Biomaterials* **2008**, *29*, 4561–4573.
(12) Schuler, M.; Trentin, D.; Textor, M.; Tosatti, S. G. P. *Nanomed.* **2009**, *1*, 449–463.
(13) Peter, B.; Pioletti, D. P.; Laib, S.; Bujoli, B.; Pilet, P.; Janvier, P.; Guicheux, J.; Zambelli, P. Y.; Bouler, J. M.; Gauthier, O. *Bone* **2005**, *36*, 52–60.
(14) Brigger, I.; Dubernet, C.; Couvreur, P. *Adv. Drug Delivery Rev.* **2002**, *54*, 631–651.
(15) Braeckmans, K.; Smedt, S. C. D.; Leblans, M.; Pauwels, R.; Demeester, J. *Nat. Rev. Drug Discovery* **2002**, *1*, 447–456.
(16) Gawalt, E. S.; Avaltroni, M. J.; Danahy, M. P.; Silverman, B. M.; Hanson, E. L.; Midwood, K. S.; Schwarzbauer, J. E.; Schwartz, J. *Langmuir* **2003**, *19*, 200–204.
(17) Aumelas, A.; Serrero, A.; Durand, A.; Dellacherie, E.; Leonard, M. *Colloids Surf., B* **2007**, *59*, 74–80.
(18) Macak, J. M.; Schmuki, P. *Electrochim. Acta* **2006**, *52*, 1258–1264.
(19) Macak, J. M.; Albu, S.; Kim, D. H.; Paramasivam, I.; Aldabergerova, S.; Schmuki, P. *Electrochem. Solid-State Lett.* **2007**, *10*, K28.
(20) Yasuda, K.; Schmuki, P. *Electrochem. Commun.* **2007**, *9*, 615–619.
(21) Albu, S.; Kim, D. H.; Schmuki, P. *Angew. Chem., Int. Ed.* **2008**, *47*, 1916.
(22) Balaur, E.; Macak, J. M.; Tsuchiya, H.; Schmuki, P. *J. Mater. Chem.* **2005**, *15*, 4488–4491.
(23) Song, Y. Y.; Hildebrand, H.; Schmuki, P. To be submitted for publication.
(24) Dorvee, J. R.; Derfus, A. M.; Bhatia, S. N.; Sailor, M. J. *Nat. Mater.* **2004**, *3*, 896–899.
(25) Tiller, J.; Berlin, P.; Klemm, D. *Biotechnol. Appl. Biochem.* **1999**, *30*, 155–162.
(26) Thomas, J. C.; Pacholski, C.; Sailor, M. J. *Lab Chip* **2006**, *6*, 782–787.
(27) Sakai, N. Y.; Fujishima, A.; Watanabe, T.; Hashimoto, K. *J. Phys. Chem. B* **2003**, *107*, 1028–1035.
(28) Stein, F. S.; Hahn, R.; Song, Y. Y.; Shrestha, N. K.; Schmuki, P. Submitted for publication.

JA810130H